JOURNAL OF MATERIALS SCIENCE 28 (1993) 3845–3850

# Cyclic deformation behaviour and morphology of polypropylene

TAKASHI ARIYAMA
*Department of Mechanical Engineering, Faculty of Engineering, Science University of Tokyo, 1-3 Kagurazaka, Shinjuku-ku, Tokyo 162, Japan*

The viscoelastic–plastic behaviour and stress relaxation in polypropylene after uniaxial simple tension or cyclic preloading are studied by an electrohydraulic, servo-controlled testing machine. The stress–strain curve data of simple tension at different strain rates show that the magnitude of stress depends strongly on strain rate. The stress relaxation behaviour after simple tension and cyclic preloading indicates complex features and reveals differences in the deformation of molecular chains in polypropylene subjected to different cyclic preloadings. The stress–strain curves and the stress relaxation curves under three mean strains are fairly different from each other. The microstructural changes in samples subjected to different cyclic preloadings were determined by scanning electron microscopy (SEM). The results of the stress–strain curves and the stress relaxation behaviour are discussed in comparison with the observation of SEM fractographs.

## 1. Introduction

The deformation behaviour of ductile polymers such as polyethylene and polypropylene is considered to show different behaviour in tension and compression. The polymers show a cyclic work-softening in cyclic preloading, including a semi-elastic deformation, and the molecular structure shows complicated features. Studies on the viscoelastic–plastic properties seem to be important to investigate the feasibility of using the polymeric materials as machinery parts or structural materials. It is reported that polypropylene exhibits an excellent fatigue resistance during large-strain cyclic deformation [1], and a ductile polymer of polycarbonate undergoes a marked decrease in deformation resistance prior to crack formation. Shinozaki and Sargent [2] reported the microstructural changes during large-strain cyclic deformation of polypropylene deformed uniaxially beyond the gross yield point and subsequently cycled into compression. They observed the appearance of a neck in tension, the disappearance of the neck as the specimen is compressed, and bulging of the specimen in the previously necked region.

On the other hand the morphology of a material influenced by the cyclic deformation process is of considerable importance from both a basic and a practical point of view. Attala *et al.* [3], in samples of isotactic polypropylene (PP) having different morphologies and crystallinities, reported that both crystallinity and spherulite size enhance the non-linearity of the viscoelastic response, and that an increase in the size of crystalline aggregates increases the values of relaxation moduli.

In the present study, the viscoelastic–plastic properties of PP, subjected to different cyclic preloadings of uniaxial tension–compression, are investigated by use of a closed-loop, electrohydraulic, servo-controlled testing machine. Stress–strain and stress relaxation tests were performed under various sets of strain rate, strain amplitude and number of cycles. The results are compared with the microstructure of the molecular chains.

## 2. Experimental procedure

### 2.1. Testing system

Stress–strain curves and stress–relaxation curves were obtained by use of a closed-loop, electrohydraulic, servo-controlled testing machine. The bottom grip was stationary while the top one moved vertically. Specimens were tested in a tension–compression mode under strain control. Applied loads were measured directly by means of a strain-gauge load cell. A new extensometer was developed for measuring strain in the rod specimen [4]. Two strain gauges were mounted on a phosphor-bronze board about 0.3 mm thick with an adhesive bond. The extensometer was attached to the specimen with two springs as knife-edges lightly contacting the specimen. Load and displacement data from each specimen were fed to a computer and stored on floppy disks after data processing. In the present work, all tests were performed under strain control at room temperature (18–23°C). A detailed description of the testing machine and the extensometer is given elsewhere [4].

### 2.2. Materials

Commercial PP, (Grade J105 manufactured by Ube

0022–2461  

Industries Ltd) was used. The crystal modification was a monoclinic α form and the melting index flow was 0.005 kg/10 min. The apparent density was 907 kg m$^{-3}$ at 18 °C. The molecular weight was 285 000, estimated from the melting index flow [5], and the degree of crystallinity was 56%, calculated from the density [6]. The mean spherulite diameter of the asreceived materials was 180 μm, as manifested by polarizing microscopy [7].

### 2.3. Sample preparation for cyclic tests

The as-received material was machined to a rod specimen with a lathe. The gauge length was 150 mm and the diameter of the straight part was 10 mm [4]. The surface of the straight part was polished on emery papers because of visible flaws and scratches. The microstructure of the straight part was homogeneous: this fact was confirmed by direct observation of the spherulite deformation by polarizing microscopy [7].

### 2.4. Conditions of cyclic loading

Table I lists the conditions of cyclic preloading. The strain rate $\dot{\varepsilon}$, number of cycles $N$ and mean strain $\varepsilon_m$ are taken as parameters. In the strain ranges used, no stress-whitening was observed by the naked eye.

### 2.5. Stress relaxation tests

The stress relaxation tests were performed under three modes, i.e. after uniaxial simple tension ($N = 0$), a number of cycles ($N = 50$), and at different mean strains ($\varepsilon_m = 0$, $+2.5$ and $-2.5$ %). The tests were made after different predetermined strain rates ($\dot{\varepsilon} = 500$, 1000 and 10 000 μ s$^{-1}$ where μ = microstrain units) at a testing time of 1200 s for all tests.

### 2.6. Scanning electron microscopy fractographs

For fractographic investigations, specimens subjected to different cyclic preloadings were immersed in liquid nitrogen at 30 min to freeze the structure; immediately after removal from the vessel they were fractured perpendicular to the tensile or compressive direction. The fractured surfaces of the specimens were then sputter-coated with gold and viewed under a scanning electron microscope (Hitachi S-2150).

## 3. Results and discussion

### 3.1. Stress–strain curves of simple tension

Fig. 1 shows the stress–strain curves for uniaxial simple tension at different strain rates $\dot{\varepsilon}$, i.e. $\dot{\varepsilon} = 50$, 500, 1000 and 10 000 μ s$^{-1}$. In the plastic range the value of stress depends strongly on strain rate, i.e. the magnitude of stress increases with increasing strain rate above the yield point (at about $\varepsilon = 0.7$ %). This behaviour is fairly different from that of some metals such as an austenitic stainless steel (SUS 304) and a ferritic 2.25 Cr–1Mo steel [8]. In these metals, the work-hardening coefficient $E_p$ is nearly constant in the plastic range and is independent of strain rate.

Fig. 2 shows the work-hardening coefficient $E_p$ versus strain rate $\dot{\varepsilon}$ as a function of strain ε. The magnitude of $E_p$ at $\varepsilon = 1$ % is larger than for other strains and increases steeply with increasing strain

TABLE I Conditions of cyclic preloading

| Mean strain $\varepsilon_m$ (%) | Number of cycles $N$ | Strain rate $\dot{\varepsilon}$(μ s$^{-1}$) |
|---|---|---|
| 0 | 50 | 1000 |
| + 2.5 | 50 | 1000 |
| − 2.5 | 50 | 1000 |

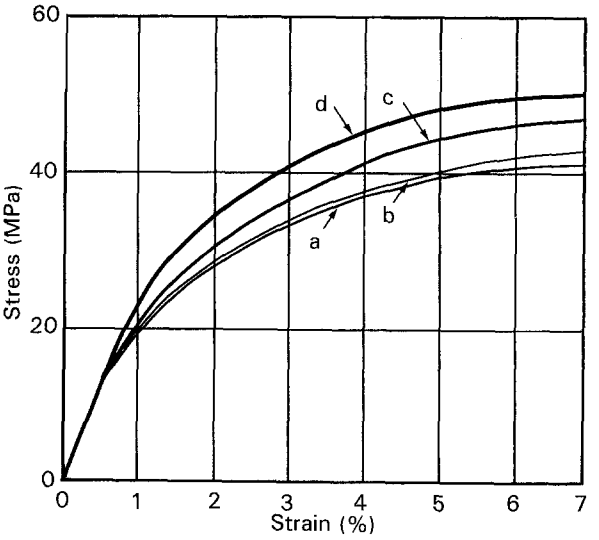


*Figure 1* Stress–strain curves for uniaxial simple tension at different strain rates: $\dot{\varepsilon}$ = (a) 50, (b) 500, (c) 1000, (d) 10 000 μ s$^{-1}$.

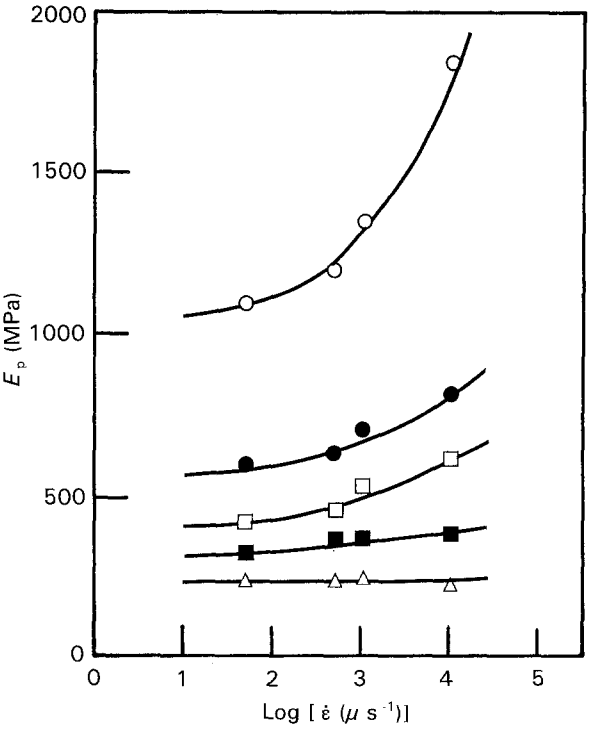


*Figure 2* Work-hardening coefficient versus strain rate as a function of strain ε = (○) 1 %, (●) 2 %, (□) 3 %, (■) 4 %, (△) 5 %.

rate. At higher strain, however, the $E_p$ value is independent of strain rate. Liu and Harrison [9] studied the effect of draw rate on the stress–strain behaviour of polymers, including polypropylene, poly(ethylene terephthalate) and polyethylene. They reported that when the draw rate is larger than a critical value, the Young's modulus and yield stress decrease rapidly with increasing draw rate; further, there is a change in the yield mechanism due to a decrease in modulus and yield stress arising from void formation and crazing.

## 3.2. Stress relaxation after cyclic preloading

The results of stress relaxation tests after simple tension ($N = 0$) and after cyclic preloading ($N = 50$) at different strain rates are shown in Fig. 3. The tests were performed on specimens which were deformed to a predetermined strain of $\varepsilon = 3\,\%$ for $N = 0$ and to a strain amplitude of $\Delta\varepsilon/2 = \pm 3\,\%$ for $N = 50$. It is observed in Fig. 3 that the relaxation curves after cyclic preloading with $N = 50$ have a similar shape. On the other hand, the curve for simple tension ($N = 0$) depends strongly on strain rate. The decrease in stress drop at $\dot{\varepsilon} = 10\,000\ \mu\ s^{-1}$ is much larger than that at $\dot{\varepsilon} = 1000\ \mu s^{-1}$. In addition, at about time $t = 600$ s the curves at $N = 50$ reach an equilibrium stress but the curves at $N = 0$ do not reach the equilibrium stress even at 1200 s. The stress drop at $\dot{\varepsilon} = 10\,000\ \mu\ s^{-1}$ decreases steeply at the beginning of the relaxation in contrast to other relaxation curves. Hence, it can be seen that the stress relaxation behaviour indicates complicated features and reveals differences in the deformation of molecular chains in PP specimens subjected to different cyclic preloadings.

Fig. 4 shows the drop of stress versus stress at the initial relaxation ($t = 0$); the magnitude of stress drop was determined at 1200 s. In all conditions of different cyclic preloading tested here, the drop of stress increases in a linear fashion with increasing stress level. The slopes of the curves are found to depend on the strain rate and the number of cycles. It is seen that the stress level affects the stress relaxation behaviour in PP subjected to cyclic preloading.

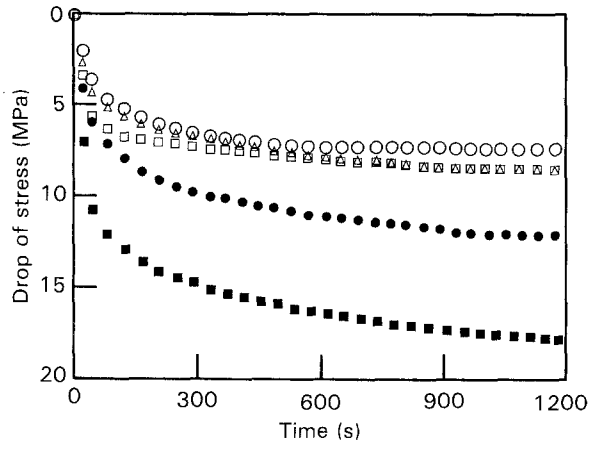


*Figure 3* Stress relaxation curves of PP after simple tension ($N = 0$) and cyclic preloading ($N = 50$) at different strain rates: (●) $N = 0$ and $\dot{\varepsilon} = 1000\ \mu\ s^{-1}$; (■) $N = 0$ and $\dot{\varepsilon} = 10\,000\ \mu\ s^{-1}$; (△) $N = 50$ and $\dot{\varepsilon} = 500\ \mu\ s^{-1}$; (○) $N = 50$ and $\dot{\varepsilon} = 1000\ \mu\ s^{-1}$; (□) $N = 50$ and $\dot{\varepsilon} = 10000\ \mu\ s^{-1}$.

## 3.3. Effects of mean strain on stress–strain curves and stress relaxation

The experimental data for stress–strain curves, under the conditions of cyclic preloading listed in Table I, are depicted in Figs 5 to 7. At a mean strain $\varepsilon_m$ of $\varepsilon_m = 0\,\%$ (Fig. 5), the stress–strain curve is fairly different from that of some metals [10], as similar behaviour is observed in simple tension (Fig. 1) and the initial stress–strain curve is very different from all subsequent curves. A slight work-softening can be seen in the initial number of cycles. The curve tends to reach a steady state as the number of cycles increases. The steady-state behaviour is seen at a number of cycles $N = 30$–$50$. These facts coincide with the results for other different strain amplitudes in PP specimens [4, 11]. In Fig. 5, an unusual propeller-like shape of the hysteresis loop is observed in the first ten cycles. The same behaviour is seen in the results of torsional tests on PP [12].

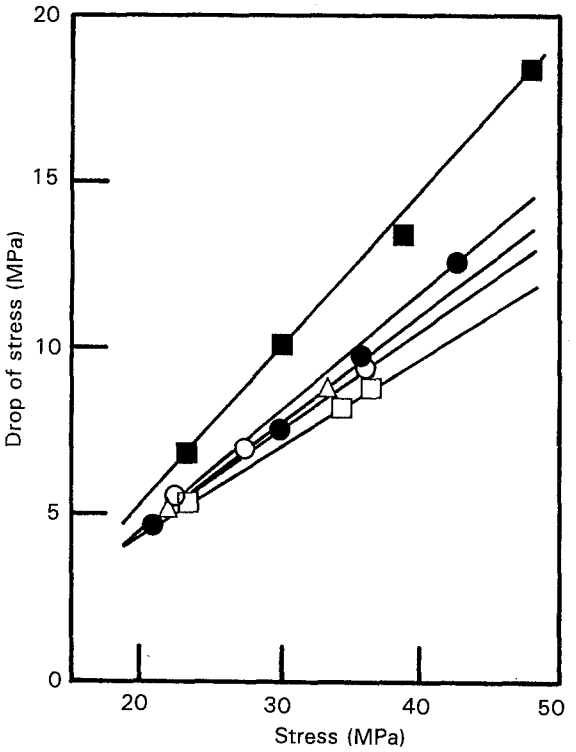


*Figure 4* Drop of stress versus stress at initial relaxation; the magnitude of stress drop was determined at 1200 s. Symbols as in Fig. 3.

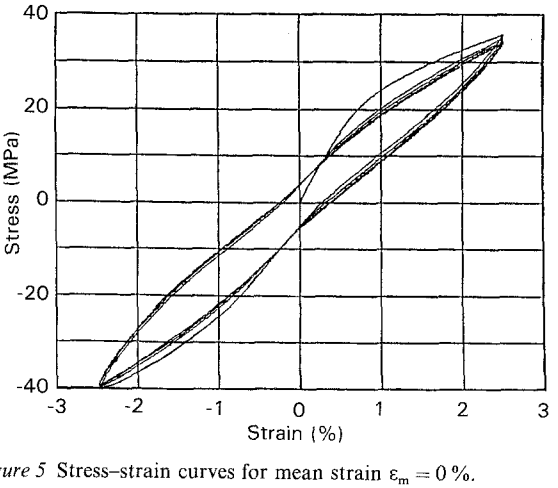


*Figure 5* Stress–strain curves for mean strain $\varepsilon_m = 0\,\%$.

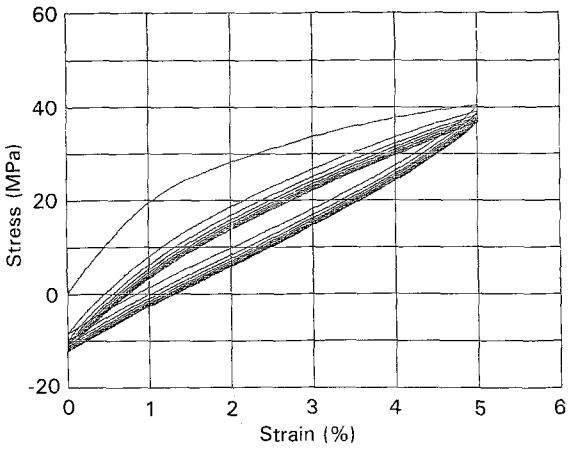


*Figure 6* Stress–strain curves for mean strain $\varepsilon_m = +2.5\,\%$.

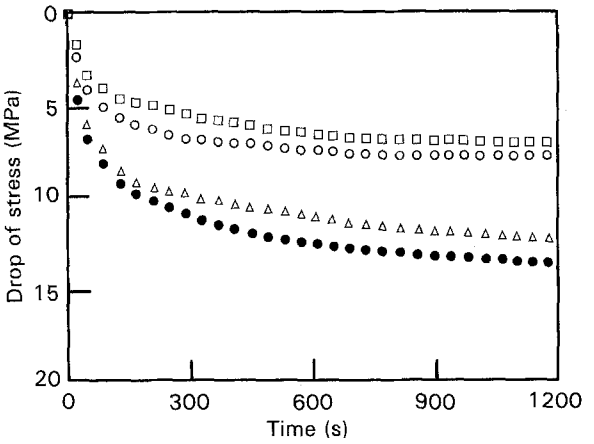


*Figure 8* Stress relaxation curves for different mean strains at a strain rate of $\dot{\varepsilon} = 1000\ \mu\ s^{-1}$ after $N = 50$: (○) $\varepsilon_m = 0\,\%$ (tension), (●) $\varepsilon_m = 0\,\%$ (compression), (□) $\varepsilon_m = +2.5\,\%$, (△) $\varepsilon_m = -2.5\,\%$.

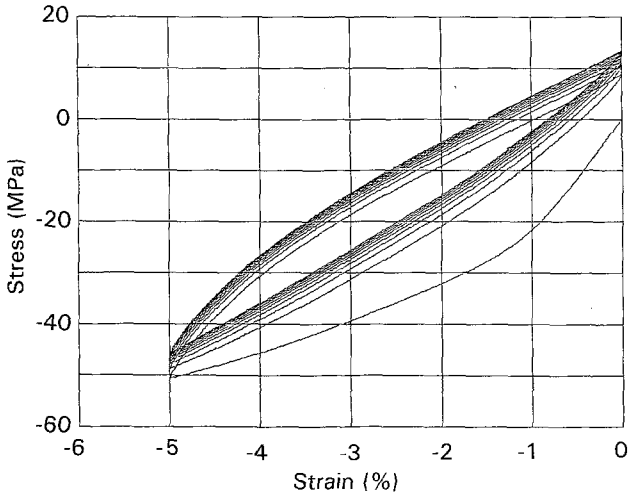


*Figure 7* Stress–strain curves for mean strain $\varepsilon_m = -2.5\,\%$.

The magnitude of the peak tensile stress is smaller at about 10 MPa than that of the peak compressive stress: i.e. the mean stress, defined as the mean of the peak tensile stress and the compressive one, is shifted to the compressive side. The hysteresis loop does not become symmetrical with respect to the origin in Fig. 5. This behaviour is different from that of torsional tests at a shear strain of 0.2 and a strain rate of $1400\ \mu\ s^{-1}$ [13]. In contrast, hysteresis loops roughly symmetrical about the tip-to-tip axis are obtained for some metals [10]. For a ductile polymer of polycarbonate, the peak stress decreases rapidly in tension and compression from one cycle to the next at a cyclic strain of about 14 % in room-temperature tests; but in liquid nitrogen tests ($-125\,°C$) the tensile peak stress decreases with increasing number of cycles in contrast to the constant compressive stress [1]. Bucknall and Stevens [14] reported that the mechanisms of fatigue damage in acrylonitrile butadiene styrene copolymer (ABS) and high-impact polystyrene (HIPS) were studied by changes in mechanical properties under sinusoidal and square-wave loading at a frequency of 0.033 Hz. They concluded that both materials exhibit a large increase in hysteresis and a decrease in modulus and that the hysteresis loop is approximately elliptical with the tensile and compressive portions similar in size and shape, while in HIPS the loop is irregular in shape.

For mean strains of $\varepsilon_m = +2.5\,\%$ (Fig. 6) and $\varepsilon_m = -2.5\,\%$ (Fig. 7), cyclic work-softening is also observed as seen for $\varepsilon_m = 0\,\%$ (Fig. 5). The magnitude of the peak stress for $\varepsilon_m = -2.5\,\%$ is larger than for $\varepsilon_m = +2.5\,\%$. On the other hand, the mean stress is shifted to the preloading direction in both cases of $\varepsilon_m = +2.5\,\%$ and $\varepsilon_m = -2.5\,\%$, and the subsequent loops distort in shape. This behaviour is fairly different from that of the case of $\varepsilon_m = 0\,\%$ (Fig. 5). It appears that the reason for the discrepancy in the results between $\varepsilon_m = 0\,\%$ and $\varepsilon_m = +2.5\,\%$ or $\varepsilon_m = -2.5\,\%$ is due to the narrower elastic range, in contrast to some metals [8], and the change of stress corresponding to the strain change is small because of the smaller hardening coefficient. The loops shift in a direction such that the mean stress approaches zero stress ($\sigma = 0$), as a result of the proceeding of cyclic preloading. It appears that the higher stress level is decreased by cyclic preloading. The stress width (peak-to-peak stress) is larger with an increase in the mean stress (or mean strain). This behaviour is due to the difference in the magnitude of the elastic coefficient $E_e$: $E_e$ is 1600 MPa at the stress level of 40 MPa for $\varepsilon_m = +2.5\,\%$, and $E_e$ is 2600 MPa at 40–50 MPa for $\varepsilon_m = -2.5\,\%$.

### 3.4. Stress relaxation behaviour at mean stress

Fig. 8 shows the stress relaxation curves listed in Table I. The stress relaxation curves for $\varepsilon_m = 0\,\%$ and $+2.5\,\%$ show the same behaviour but the stress levels are different. The curve for $\varepsilon_m = -2.5\,\%$ is different from that for $\varepsilon_m = 0\,\%$ and $+2.5\,\%$, and does not reach the equilibrium stress even at 1200 s. Hence, the behaviour of the stress–strain and stress relaxation results seems to be due to microstructural changes in the molecular chains.

### 3.5. Microstructural changes

Figs 9–12 shows SEM fractographs of the as-received PP and specimens subjected to the different cyclic

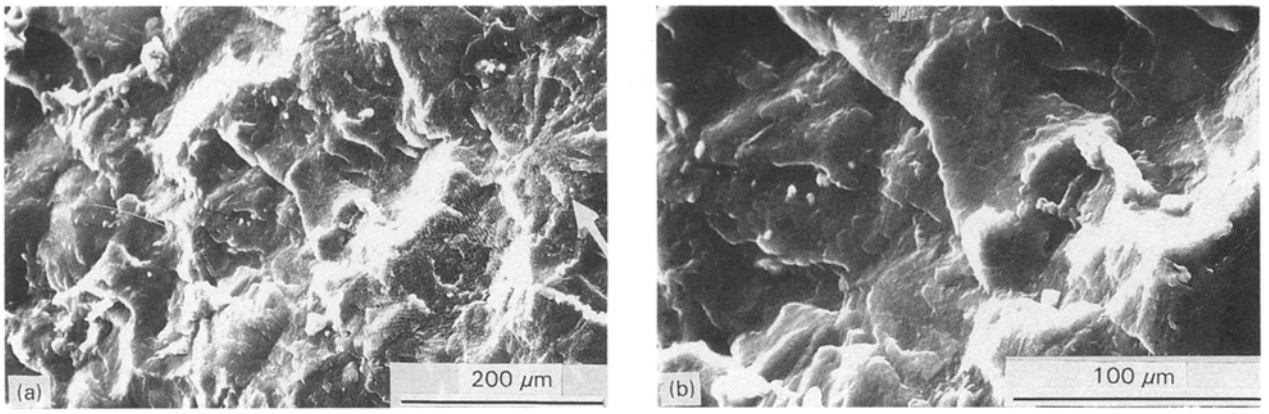


*Figure 9* (a, b) SEM fractographs of as-received PP.

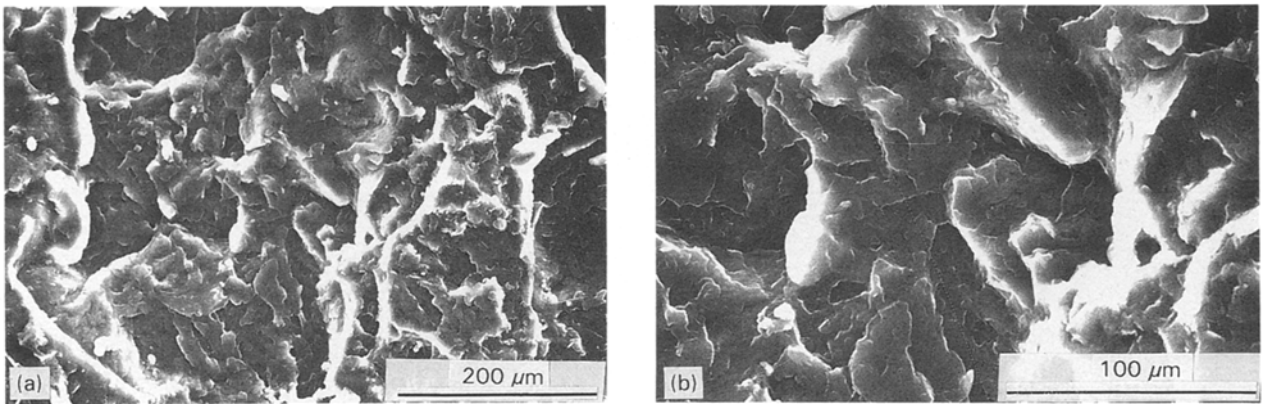


*Figure 10* (a, b) SEM fractographs for mean strain $\varepsilon_m = 0\,\%$.

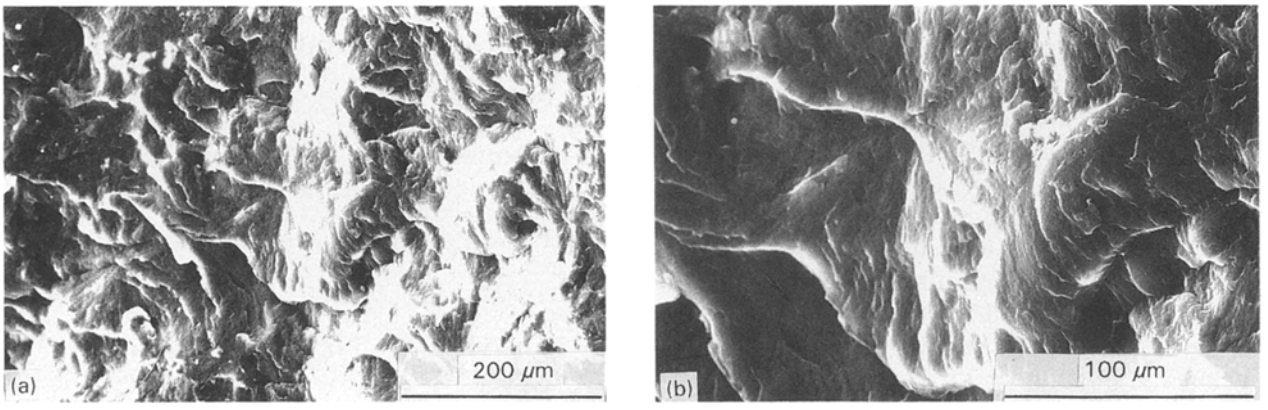


*Figure 11* (a, b) SEM fractographs for mean strain $\varepsilon_m = +2.5\,\%$.

preloadings listed in Table I. The fracture surface is perpendicular to the longitudinal direction of the specimen (the direction of cyclic preloading). As clearly seen in Fig. 9a, the as-received sample has comparatively large spherulites and the diameter of the spherulites was about 180 μm (indicated by an arrow in Fig. 9a). Supporting evidence is shown in Fig. 9b, which presents a high-magnification SEM micrograph of the central domain in Fig. 9a. The as-received PP sample is essentially isotropic, as manifested by wide-angle X-ray diffraction and polarizing microscopy [4]. The lamella radiates outward from the centre of the spherulite.

In the sample with $\varepsilon_m = 0\,\%$, the lamellar structure is broken up and the spherulites have entirely disappeared, as clearly seen in Fig. 10a. This fractograph is significantly different from that of the as-received PP. It appears in Fig. 10b that cracks are observed in each lamella.

On the other hand, in the sample with $\varepsilon_m = +2.5\,\%$ (Fig. 11a) spherulites are again observed, just as in the as-received sample, but the lamella is twisted

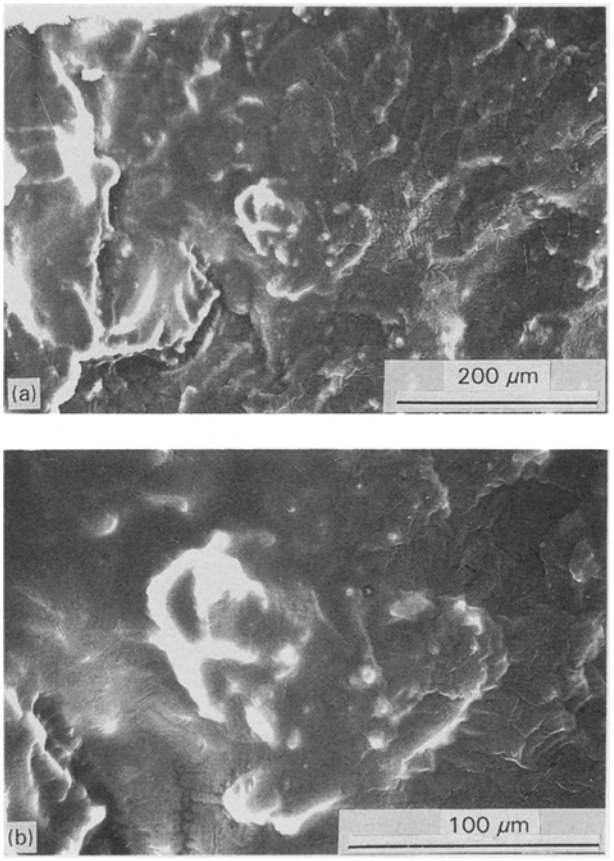


*Figure 12* (a, b) SEM fractographs for mean strain $\varepsilon_m = -2.5\,\%$.

from the centre of the spherulite (Fig. 11b). Cracks are not observed in these twisted lamellae. This behaviour is a significant characteristic. As shown in Fig. 12a and b, neither spherulites nor lamellae can be found in the sample with $\varepsilon_m = -2.5\,\%$. The overall microstructure shows a "molten" state in contrast to the molecular structure for other mean strains and the as-received PP. This fact indicates that the lamellae are fairly broken up when the sample is subjected to cyclic compressive preloading. In PP specimens deformed uniaxially beyond the gross yield point and subsequently cycled into compression (elongation between the limits + 1.067 and − 0.267 cm), the observation of deformed spherulites in the necked region indicates that the cold-drawing process is but a continuation of plastic deformation behaviour prior to the gross yield point, and a feature of the deformed microstructure is the appearance of cracks (or crazes) normal to the tensile axis in longitudinal sections of the spherulites [2]. These results were obtained from tests with large-strain cyclic deformation in contrast to the results reported here. Hence, it is concluded from the results of the stress–strain curves, stress relaxation curves and SEM fractographs that significant microstructural changes of PP molecular chains occur under different cyclic preloadings.

## 4. Conclusions

The stress–strain curves of polypropylene after simple tension indicate that the magnitude of the stress above the yield point (above a strain of 0.7 %) depends strongly on strain rate. Relaxation tests after simple tension and after cyclic preloading show different behaviour; the decrease in stress drop at $\dot{\varepsilon} = 10\,000\ \mu\,s^{-1}$ is much larger than that at $\dot{\varepsilon} = 1000\ \mu\ s^{-1}$ and the relaxation curve for simple tension depends on strain rate. From the results for the drop of stress versus stress at initial relaxation, it is seen that the drop of stress increases in a linear fashion with increasing stress level; the stress level affects the relaxation behaviour in PP samples subjected to cyclic preloading. The stress–strain curves at three mean strains indicate different loop behaviour. For a mean strain of $\varepsilon_m = 0\,\%$ the magnitude of the peak tensile stress is smaller by about 10 MPa than that of the peak compressive stress, and the mean stress is shifted to the compressive side. On the other hand, for $\varepsilon_m = +2.5\,\%$ and $\varepsilon_m = -2.5\,\%$ the mean stress is shifted in the preloading direction. SEM fractographs were obtained for three samples subjected to different mean strains, along with the as-received PP samples. The fractographs show different behaviour: the lamella for $\varepsilon_m = +2.5\,\%$ is twisted from the centre of the spherulite, while at $\varepsilon_m = 0\,\%$ the lamellar structure is broken up and the spherulites have entirely disappeared. For $\varepsilon_m = -2.5\,\%$, neither spherulites nor lamellae can be found and the lamellae are fairly broken up. Hence, it is concluded from the results of the stress–strain curves, stress relaxation curves and SEM fractographs, that significant microstructural changes occur under cyclic preloading.

## Acknowledgements

The author is indebted to Professor K. Kaneko, Dr M. Takenaga and Dr H. Yumoto for helpful discussion throughout these studies and also to Mr M. Sakuma and Mr K. Sakamoto for encouragement and suggestions.

## References

1. S. RABINOWITZ and P. BEARDMORE, *J. Mater. Sci.* **9**, (1974) 81.
2. D. M. SHINOZAKI and C. M. SARGENT, *ibid.* **15**, (1980) 1057.
3. G. ATTALA, I. B. GAUNELLA and R. E. COHEN, *Polym. Eng. Sci.* **23** (1983) 883.
4. T. ARIYAMA, M. TAKENAGA, K. YAMAGATA, A. KASAI and K. KANEKO, *Rep. Prog. Polym. Phys. Jpn.* **33**, (1990) 311.
5. P. PARRINI, *Macromol. Chem.* **38**, (1960) 27.
6. G. FARROW, *Polymer* **2**, (1960) 409.
7. T. ARIYAMA and M. TAKENAGA, *Polym. Eng. Sci.* **31**, (1991) 1101.
8. K. KANEKO and T. ARIYAMA, *Int. J. Plasticity* **5**, (1989) 421.
9. T. LIU and I. R. HARRISON, *Polymer* **29**, (1988) 233.
10. R. W. LANDGRAF, in ASTM STP **467**, (1970) p. 3.
11. T. ARIYAMA, *Polym. Eng. Sci.* **33** (1993) 18.
12. M. KITAGAWA, T. MORI and T. TOMOHIKO, *J. Polym. Sci. B: Polym. Phys.* **27**, (1989) 85.
13. F. De CANDIA, G. ROMANO, R. RUSSO and V. VITTORIA, *Coll. Polym. Sci.* **265**, (1987) 696.
14. C. B. BUCKNALL and W. W. STEVENS, *J. Mater. Sci.* **15** (1980) 2950.

*Received 27 February*
*and accepted 8 December 1992*